

Patterned chaos in a system of three coupled identical unidirectional ring lasers

J JOSE and S DUTTA GUPTA

School of Physics, University of Hyderabad, Hyderabad 500 134, India

MS received 10 November 1994

Abstract. Three coupled identical unidirectional B-type ring lasers are considered and the dynamics for varying coupling parameter investigated. For given system parameters like pumping, cavity damping etc. the system is characterized by three distinct types of steady states. The linear stability of these steady states is investigated in detail which are unstable beyond a critical value of the coupling parameter. For a certain range of the coupling parameter chaotic behaviour of the system is demonstrated. The dynamical variables are mapped on to a complex variable reflecting the symmetry of the system. The plot of the real vs. the imaginary part of this complex variable exhibits patterns with threefold symmetry. The largest Lyapunov exponent as well as the power spectra corresponding to the chaotic attractors are also calculated.

Keywords. Coupled ring laser; chaotic dynamics.

PACS No. 42.65

In recent years there has been a lot of interest in coupled lasers [1,2]. Studies on coupled laser systems were motivated by the fact that by means of coupling one can relatively simply increase the output power. Very recently a very different aspect of coupled identical systems has been reported. The inherent symmetries of such systems can lead to symmetric chaos [3]. Namely, in a dynamical system with symmetry, chaotic attractors may themselves possess a degree of symmetry. The symmetry aspects of three coupled identical oscillators were investigated in detail by Ashwin *et al* [4]. An almost simultaneous experiment by Ashwin [5] confirmed the theoretical predictions. However, to the best of our knowledge, similar concepts have not yet been tested for optical systems. In this paper we concentrate on an optical system with inbuilt cyclic permutation symmetry. Namely, we consider three identical unidirectional ring lasers. The choice of lasers as the constitutive element is obvious since they are known to lead to a variety of dynamical behaviour including self pulsing [6] and chaos [7]. We restrict our attention only to B-type lasers. It is well known that an isolated B-type laser is essentially a two dimensional system, and by virtue of Poincare-Bendixson theorem cannot exhibit chaotic dynamics. First ever demonstration of chaotic dynamics in such lasers was achieved by modulating the cavity damping of the lasers [8]. Later, insertion of phase sensitive elements in such laser cavities was shown to lead to additional attractors [9]. In the context of the problem of coupled B-type lasers, the important questions that can be addressed are the following: a) can coupling lead to chaotic dynamics when the individual isolated components show regular dynamics, b) does the attractor reflect the symmetries of the system after proper mapping of

the dynamical variables. It is quite clear that since the dimension of the coupled system is now higher, chaos is not ruled out. In order to provide answer to the above questions we proceed in a systematic fashion, first by looking at the steady states and investigating their linear stability. The coupling parameter is used as the control parameter and the change of stability is investigated as the coupling strength is varied. We show that beyond a critical value of the coupling parameter, all the steady states become unstable. In the domain where the steady states are unstable we integrate the equations of motion numerically. We show the existence of a window in the values of the coupling strength where the system exhibits chaotic response. In order to have direct evidence of the chaotic dynamics, we calculate the largest Lyapunov exponent and show its positivity. Moreover, we look at the power spectra which shows broad band features. To extract the symmetry features of the chaotic attractor, following ref. [4] we construct a complex dynamical variable which retains the symmetry of the system. The depiction of the variable on the complex plane exhibits the symmetries of the attractor.

Consider a system of three coupled B-type ring lasers. The lasers are assumed to be identical and unidirectional such that the output of the second laser is fed to the first and that of first is fed to the third and so on. Such a system can be described by the following set of equations [9, 1]

$$\frac{de_1}{d\tau} = -\bar{\kappa}[e_1(1 - d_1) + \beta e_2], \tag{1}$$

$$\frac{de_2}{d\tau} = -\bar{\kappa}[e_2(1 - d_2) + \beta e_3], \tag{2}$$

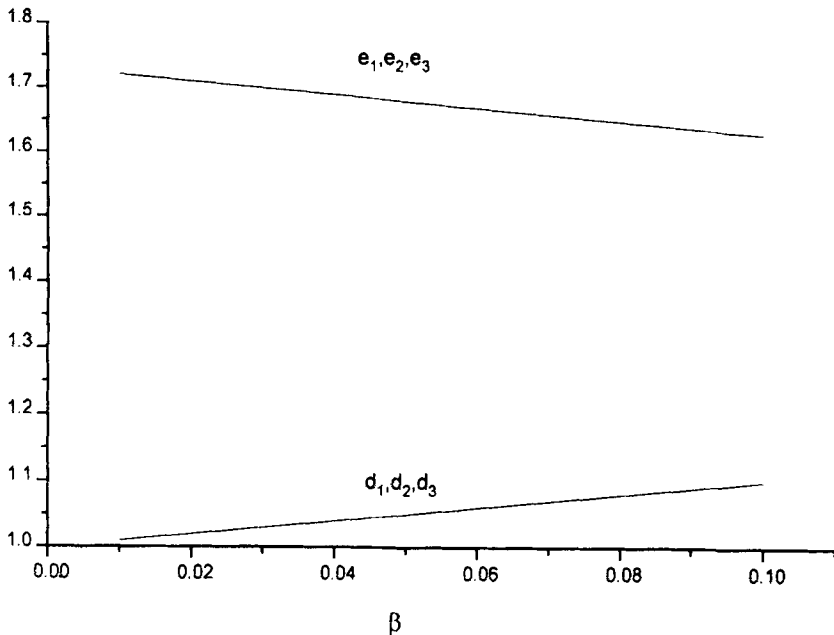


Figure 1. Steady state values of $e_j, d_j (j = 1, 3)$ as functions of coupling parameter β . The state depicting equal field and inversion for all the lasers. Parameters used for calculation are as follows: $\kappa = 100, d_0 = 4.0$.

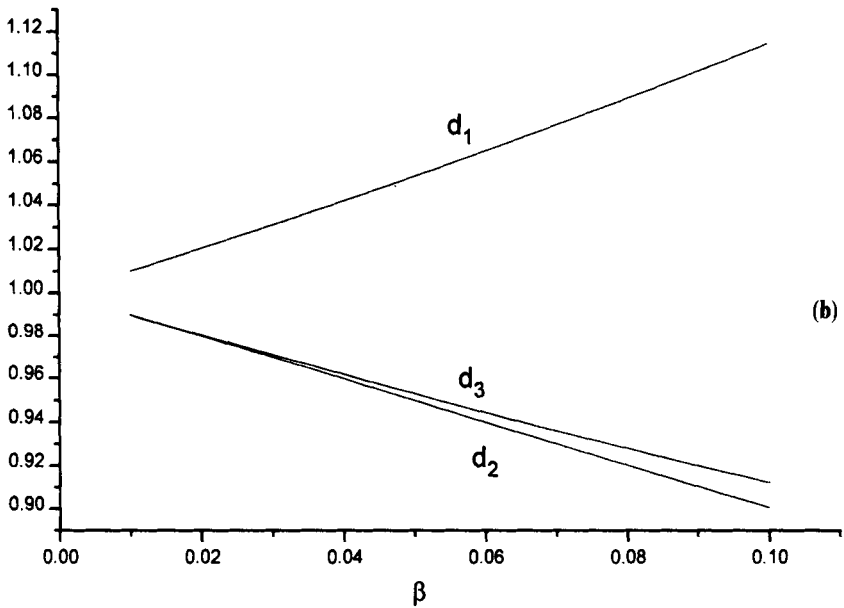
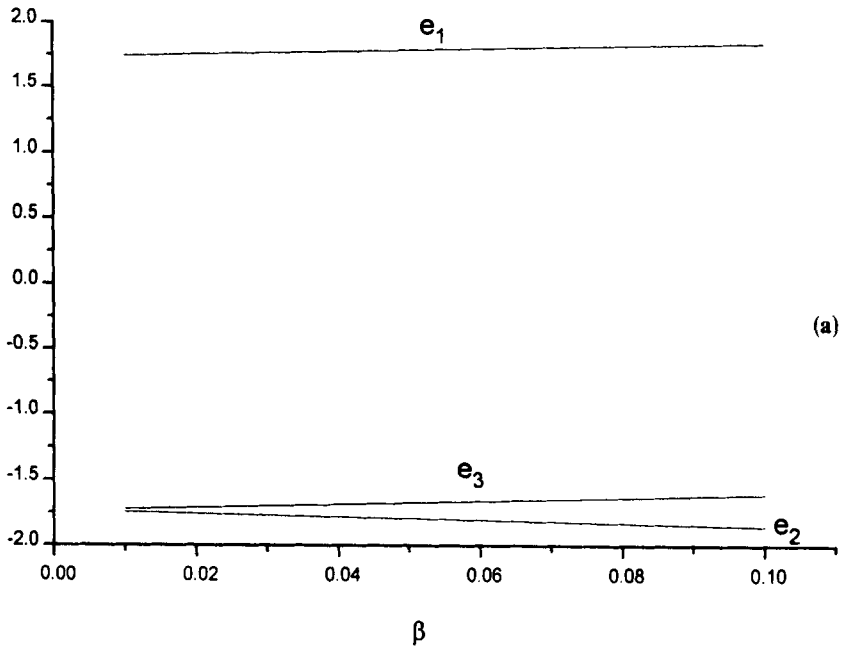


Figure 2. Steady state values of (a) e_j and (b) d_j , ($j = 1, 3$), when all the three lasers have distinct fields and inversion. Other parameters are as in figure 1.

$$\frac{de_3}{d\tau} = -\bar{\kappa}[e_3(1 - d_3) + \beta e_1], \quad (3)$$

$$\frac{dd_i}{d\tau} = -[d_j - d_0 + e_j^2 d_j], \quad j = 1, 2, 3 \quad (4)$$

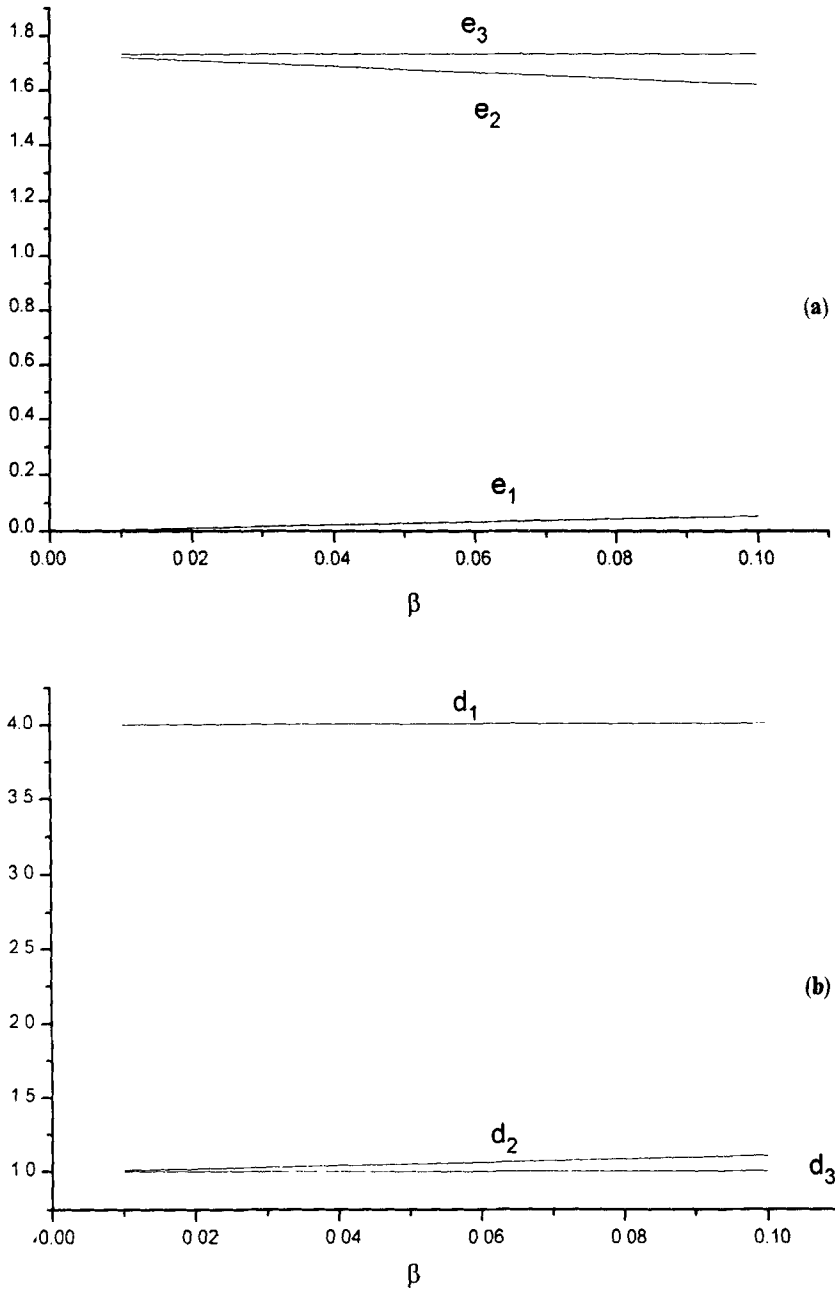


Figure 3. Steady state values of (a) e_j and (b) $d_j(j = 1, 3)$, when one of the lasers is almost off. Other parameters are as in figure 1.

where, $\bar{\kappa} = \kappa/\gamma_{\parallel}$, is the normalized (to longitudinal decay rate γ_{\parallel}) cavity damping $\tau = \gamma_{\parallel} t$ is the dimensionless time, and β is the coupling parameter. In all our calculations we have assumed β to be real for simplicity. In (1)–(4), e_j (d_j) denotes the dimensionless field envelope (inversion) of the j th laser. e_j s, for example, are normalized to the saturation amplitude, whereas, d_j s are normalized to the corresponding steady

Unidirectional ring lasers

state value of an isolated B-type system. Note also the invariant character of the system (1)–(4) under cyclic permutation of the indices 1,2,3.

We first look at the steady states and investigate their linear stability. The steady states are obtained by setting the time derivative to be zero in (1)–(4). One of the steady states, trivially obtained, is given by the following:

$$\bar{d}_j = 1 + \beta, \tag{5}$$

$$\bar{e}_j^2 = \frac{d_0}{1 + \beta} - 1. \tag{6}$$

In (5) and (6) overbars denote the steady states. The steady states given by (5) and (6) represent the state of the system where all the three lasers have the same amplitude as well as inversion. Unfortunately other steady states could not be obtained by simple analytical methods. We resorted to numerical methods in order to obtain the other steady states of the system. The results for all the steady states are shown in figures 1–3. In these figures we have plotted the different possible steady state values of e_j and $d_j(j = 1-3)$ as functions of the coupling parameter β which was varied in the range 0.01 to 0.10. For numerical calculations we have chosen the other parameters as follows: $d_0 = 4.0, \bar{\kappa} = 100$. It is clear from figures 1–3 that three distinct types of

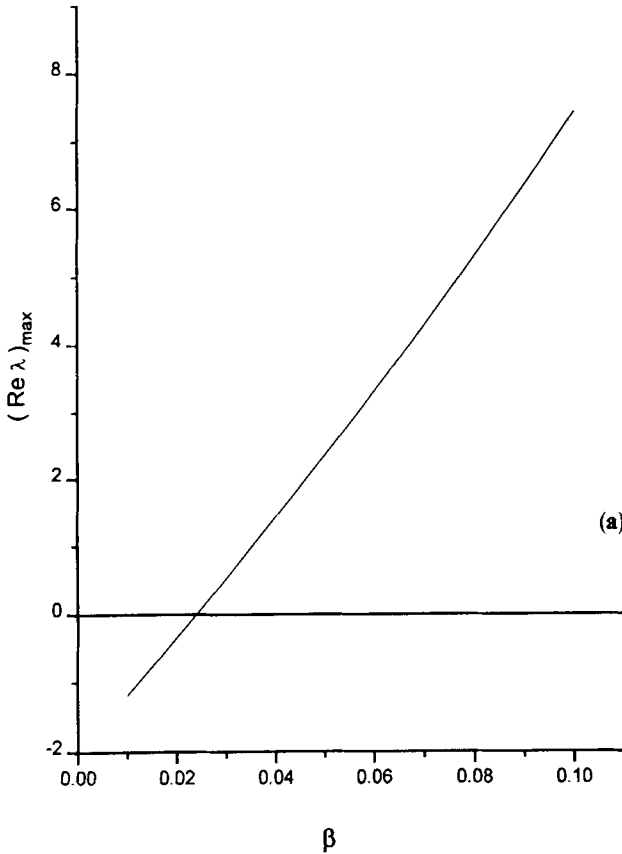


Figure 4a.

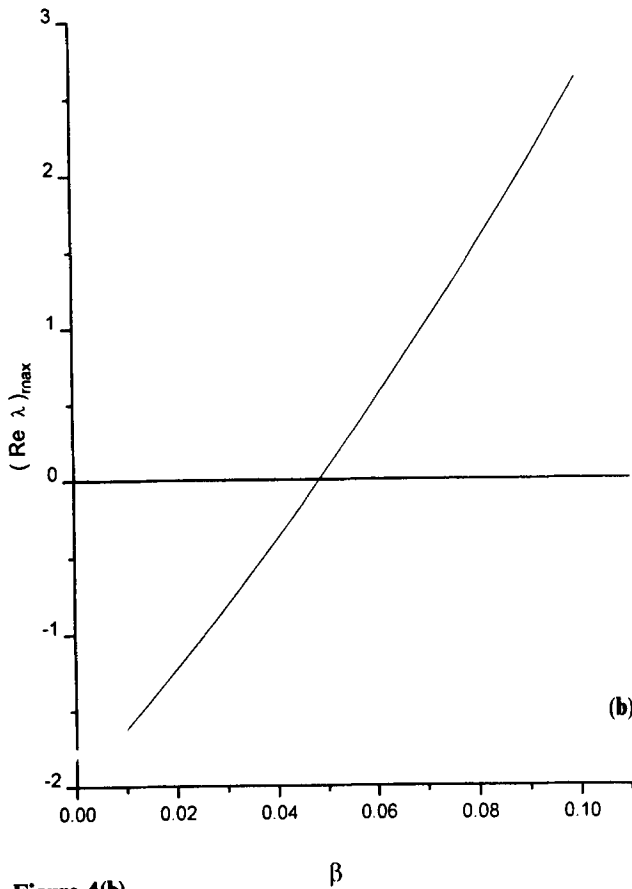


Figure 4(b).

Figure 4. Largest positive real part $[\text{Re}(\lambda)]_{\text{max}}$ of the eigenvalues of matrix A (see eq. (9)) for the steady state depicted (a) in figure 1 and (b) in figure 2.

steady states are possible. The first one is characterized by equal fields and inversions for each laser. The second one is characterized by all three lasers oscillating with non zero and distinct amplitudes (figures 2a and 2b), whereas, the third one depicts the situation when two lasers are on with the third laser close to the zero field state (figures 3a and 3b). Note that inversion corresponding to the almost “off” laser is slightly perturbed from the d_0 value meaning thereby that the initial inversion remains unburnt. Note also that similar results hold when the indices are permuted in a cyclic fashion (i.e. 1,2,3 \rightarrow 2,3,1 \rightarrow 3,1,2). In what follows we present results pertaining to the linear stability of the solutions. The temporal evolution of small perturbations around the steady state values can be described by the following equation:

$$\frac{d(\delta X)}{d\tau} = A \delta X, \tag{7}$$

where δX represents the column vector of perturbations

$$\delta X = (\delta e_1, \delta e_2, \delta e_3, \delta d_1, \delta d_2, \delta d_3)^T \tag{8}$$

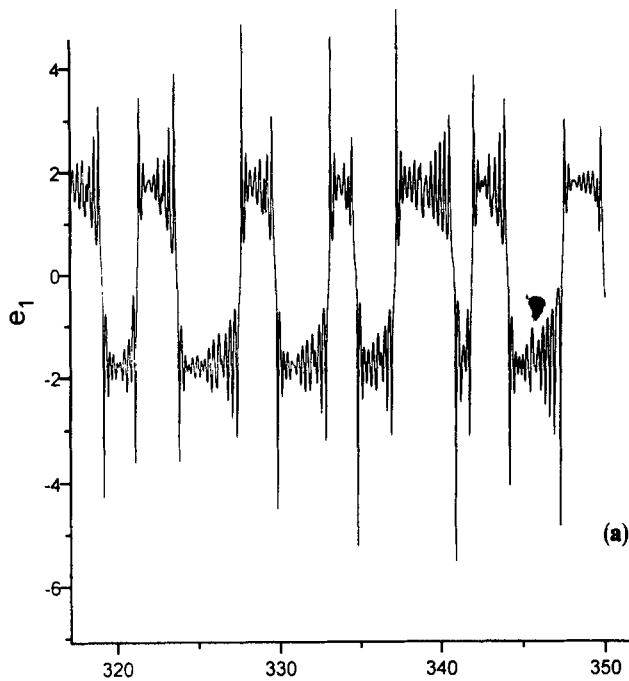


Figure 5a.

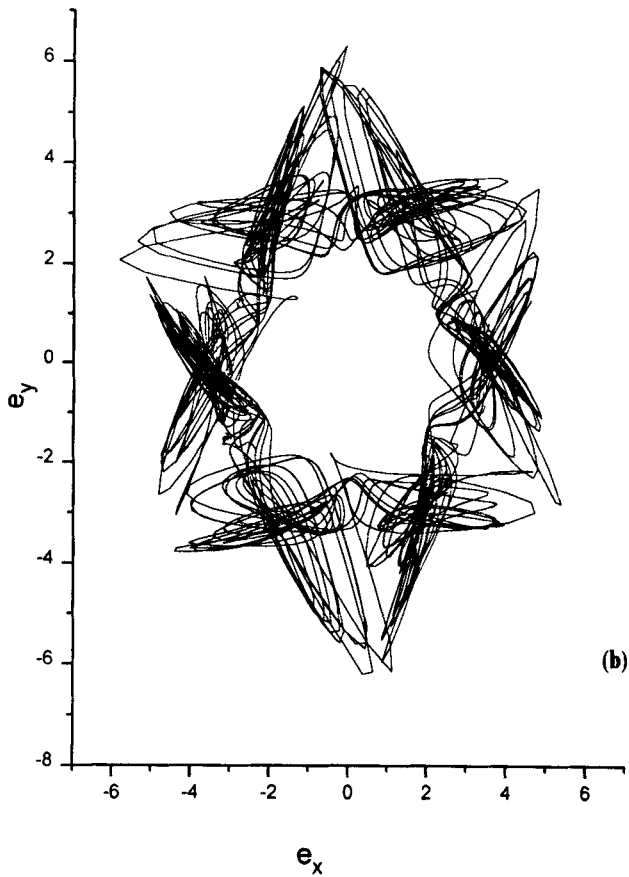


Figure 5b.

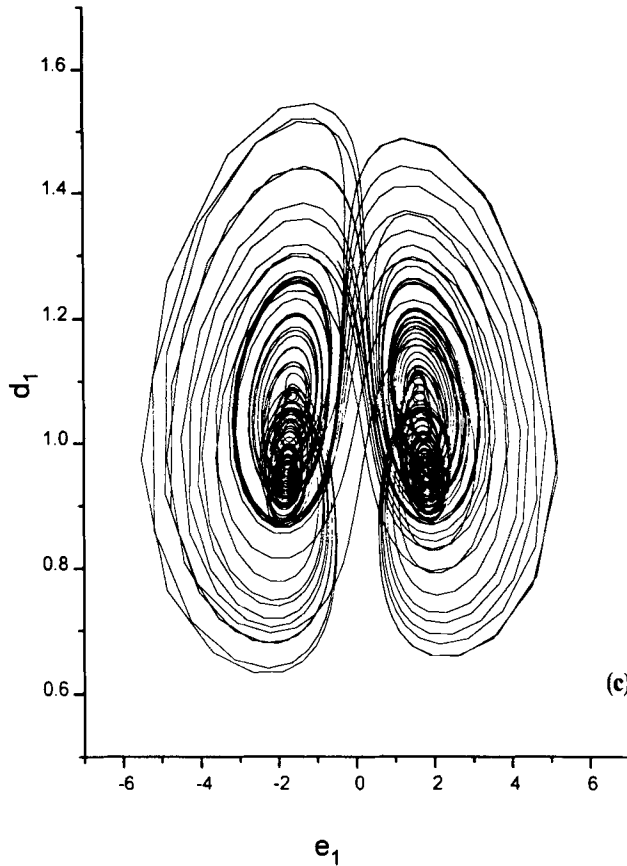


Figure 5. (a) e_1 as a function of dimensionless time τ , (b) e_y as a function of e_x and (c) e_1 as a function of d_1 for $\beta = 0.05$. Other parameters are as in figure 1.

and the matrix A is given by

$$\begin{bmatrix} -\bar{\kappa}(1 - \bar{d}_1) & -\bar{\kappa}\beta & 0 & \bar{\kappa}\bar{e}_1 & 0 & 0 \\ 0 & -\bar{\kappa}(1 - \bar{d}_2) & -\bar{\kappa}\beta & 0 & \bar{\kappa}\bar{e}_2 & 0 \\ -\bar{\kappa}\beta & 0 & -\bar{\kappa}(1 - \bar{d}_3) & 0 & 0 & \bar{\kappa}\bar{e}_3 \\ -2\bar{e}_1\bar{d}_1 & 0 & 0 & -(1 + \bar{e}_1^2) & 0 & 0 \\ 0 & -2\bar{e}_2\bar{d}_2 & 0 & 0 & -(1 + \bar{e}_2^2) & 0 \\ 0 & 0 & -2\bar{e}_3\bar{d}_3 & 0 & 0 & -(1 + \bar{e}_3^2) \end{bmatrix} \quad (9)$$

The real part of the eigenvalues of matrix A determines whether the steady state under consideration is stable or not. Presence of the positive real part of any eigenvalue heralds the instability of the fixed point. We have calculated numerically the eigenvalues of the matrix A for all steady states. We have extracted the largest real part of the eigenvalues and investigated their dependence on the coupling parameters. The results are shown in figures 4a and 4b. Figure 4a, for example, depicts the stability aspect of the steady state solution of figure 1a. It is clear from figure 4a that with an

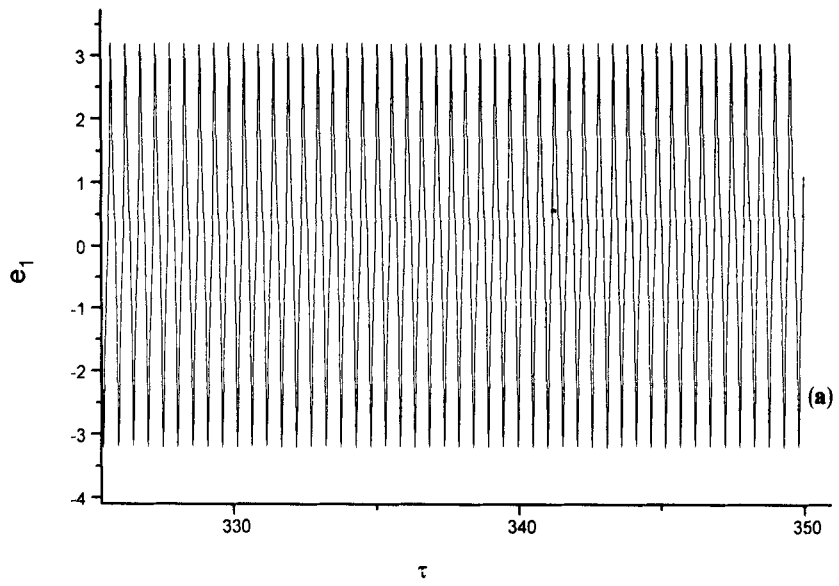


Figure 6a.

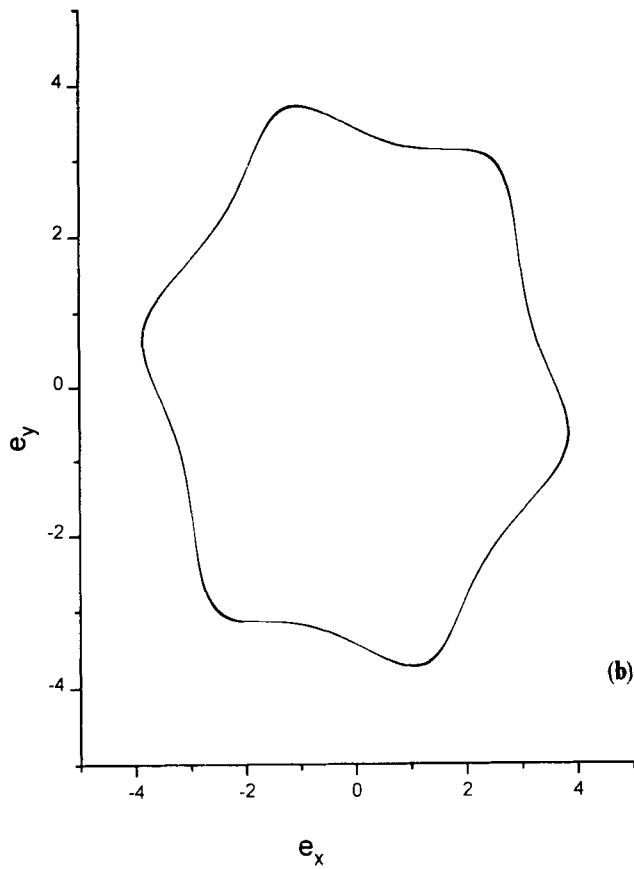


Figure 6b.

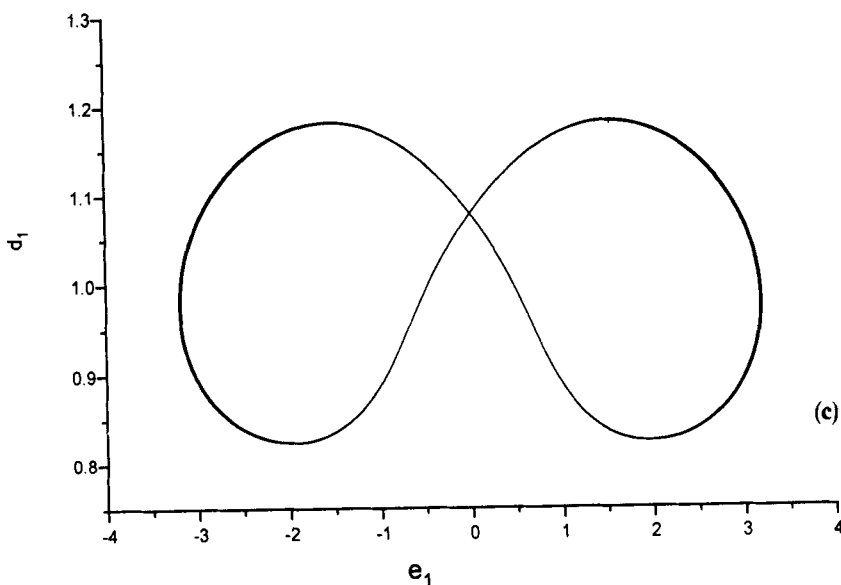


Figure 6c. Same as in figure 5 except that now $\beta = 0.069$.

increase in β the largest real part of eigenvalue $[\text{Re}(\lambda)]_{\text{max}}$ increases from negative values crossing zero at about $\beta = 0.024$. Thus the state of equal fields and equal inversion for all the lasers becomes unstable when β crosses this value. The stability results for the steady state depicted in figures 2a and 2b are given in figure 4b and these steady states become unstable when β exceeds the value 0.046. So far as the other type of steady states (with one of the lasers almosts off) is concerned, it is unstable over the range of β values considered. Thus for $\beta > 0.046$ no stable fixed points exist and the system exhibits a richer temporal dynamics.

In the domain where there are no stable fixed points we integrated the set of equations (1)–(4) numerically. Caution was taken in view of the stiff character of the equations. In order to see the symmetry aspects of the attractor following [4], we constructed a complex dynamical variable e as follows:

$$e = e_1 \exp(2\pi i/3) + e_2 \exp(4\pi i/3) + e_3. \tag{10}$$

The imaginary part e_y of e as a function of the real part e_x reflects the inherent symmetries of the dynamics. In our numerical calculation we used a wide range of values of β . For a range of β values namely $0.049 \leq \beta \leq 0.054$ chaotic dynamics was observed in the system. Below and above this window the dynamics was predominantly quasi periodic or periodic. In figure 5 we have shown the case corresponding to well developed chaos for $\beta = 0.05$. In figure 5a we have shown the temporal evolution of the field in one of the lasers. Figure 5b shows e_y as a function of e_x , whereas in figure 5c e_1 is plotted as a function of d_1 . The three-fold symmetry of the attractor shown in figure 5b is easily noticed. In order to compare with the regular

Unidirectional ring lasers

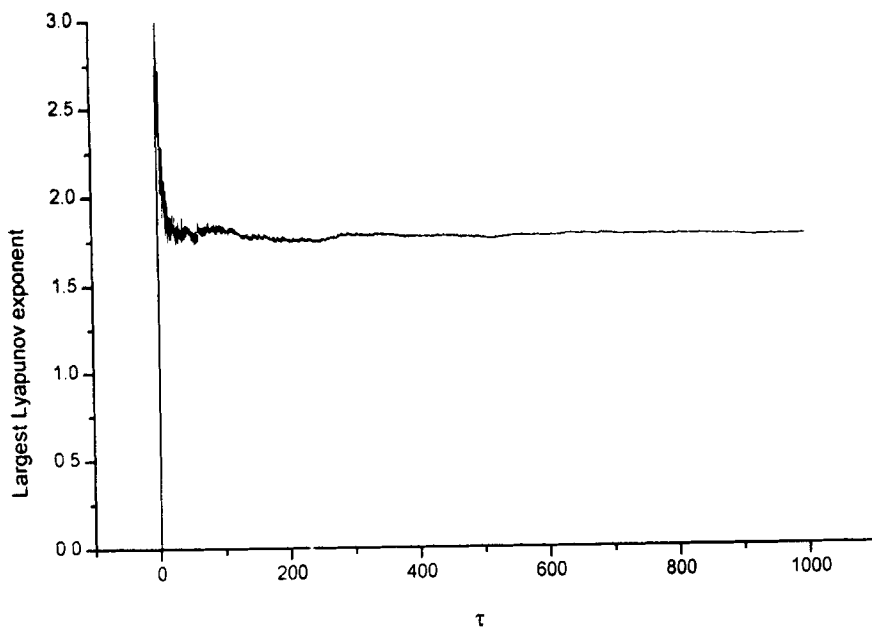


Figure 7. Convergence of largest Lyapunov exponent for $\beta = 0.05$.

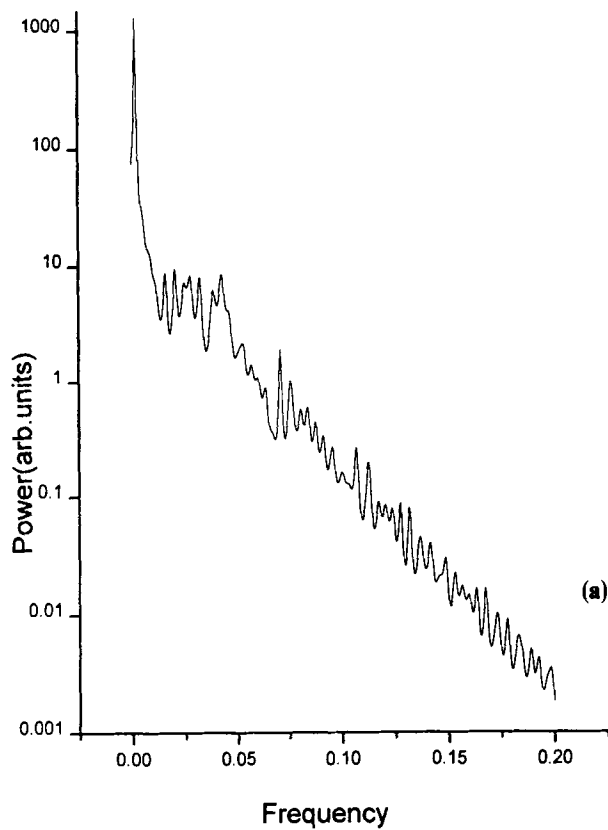


Figure 8a.

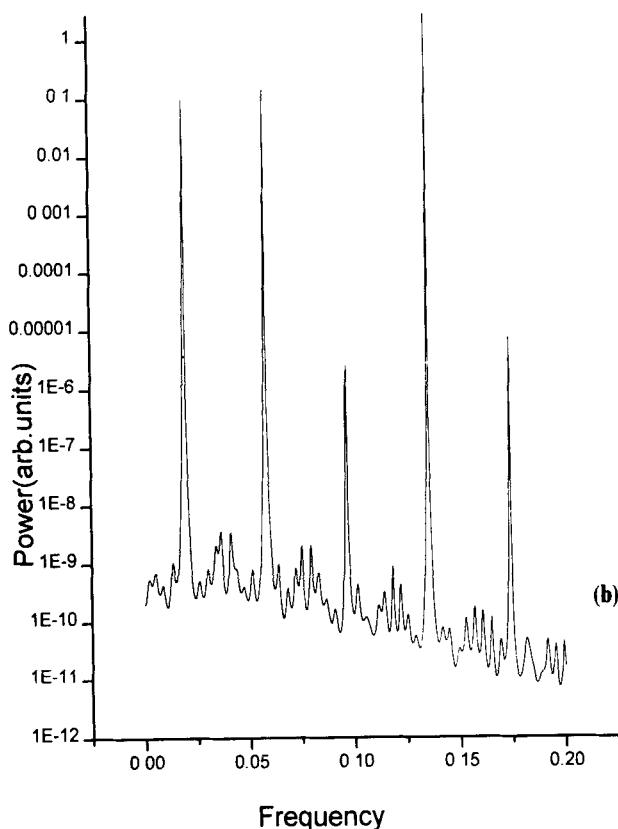


Figure 8(b).

Figure 8. Power spectrum for (a) $\beta = 0.05$ and (b) $\beta = 0.069$. Other parameters are as in figure 1.

dynamics we have also produced the curves for $\beta = 0.069$. It is clear from figures 6a–c that the temporal dynamics is periodic for $\beta = 0.069$. We have also investigated the effect of negative values of coupling. Negative coupling has a stabilizing effect on the system and all the lasers after some relaxation oscillations settle down to the steady state values.

In order to have a convincing evidence of the chaotic behaviour of the system for example, for $\beta = 0.05$ we calculated the largest Lyapunov exponent. The results are shown in figure 7 which demonstrates the convergence of the largest exponent to the value 1.74. The positive character of the largest Lyapunov exponent is a convincing proof of the chaotic dynamical behaviour of a system for $\beta = 0.05$. We have also calculated the power spectra by maximum entropy method [10] corresponding to the chaotic and the regular attractor in the positive Nyquist interval. The results corresponding to the chaotic (regular) attractor of figure 5 (figure 6) are shown in figure 8a (figure 8b). The broad band features in the chaotic case (figure 8a) are easily distinguished from the spiked ones (figure 8b) corresponding to the regular dynamics.

In conclusion, we have carried out a detailed investigation of three coupled identical ring lasers. We have shown that though the individual isolated lasers are incapable of exhibiting chaotic dynamics, the same is possible in the coupled system. With proper

mapping of the dynamical variables the attractor reflects the inherent symmetries of the system. We have carried out a detailed study of the steady states (fixed points) of the system. We have also characterized the attractors by calculating the largest Lyapunov exponent as well as the power spectra. There are still some open questions. We could not find a definitive answer as regards the route to chaos. Moreover, deviation from real character of the coupling constant complicates the problem to a large extent and phase of the coupling constant may play a significant role in determining the dynamics. These questions are under investigation and will be reported elsewhere.

Acknowledgements

One of the authors (SDG) is thankful to the Department of Science and Technology for supporting this work. He is also thankful to Prof. M Lakshmanan for bringing to his notice refs [4] and [5] which motivated this work.

References

- [1] V V Likhanskii and A P Napartovich, *Usp. Fiz. Nauk* **160**, 101 (1990)
- [2] P Mandel and L Ruo-ding, *Phys. Rev.* **A39**, 2502 (1989)
- [3] G King and L Stewart, In '*Nonlinear equations in the Applied Sciences*', edited by N F Ames and C Rogers (Academic, New York, 1992) p. 257
- [4] P Ashwin, G P King and J W Swift, *Nonlinearity*, **3**, 585 (1990)
- [5] P Ashwin, *Nonlinearity*, **3**, 603 (1990)
- [6] H Risken and K Nummedal, *Phys. Lett.* **A26**, 275 (1968)
- [7] H Haken, *Phys. Lett.* **A53**, 77 (1975)
- [8] F T Arecchi, R Meucci, G P Puccioni and J R Tredicce, *Phys. Rev. Lett.* **49**, 1217 (1982)
- [9] S Dutta Gupta and M B Pande, *J. Mod. Opt.* **39**, 1643 (1992)
- [10] *Numerical recipes, the art of scientific computing*. edited by W H Press, B P Flannery, S T Teukolsky and W T Vetterling (Cambridge University Press, Cambridge, 1986) p. 420